

UC Berkeley

UC Berkeley Previously Published Works

Title

In Vitro Spoilation of Silicone-Hydrogel Soft Contact Lenses in a Model-Blink Cell

Permalink

<https://escholarship.org/uc/item/2xd6c82z>

Journal

Optometry and Vision Science, 92(7)

ISSN

1040-5488

Authors

Peng, Cheng-Chun
Fajardo, Neil P
Razunguzwa, Trust
[et al.](#)

Publication Date

2015-07-01

DOI

10.1097/opx.0000000000000625

Peer reviewed

In Vitro Spoilation of Silicone-Hydrogel Soft Contact Lenses in a Model-Blink Cell

Cheng-Chun Peng*, Neil P. Fajardo†, Trust Razunguzwa*, and Clayton J. Radke*

*PhD † MS — Department of Chemical and Biomolecular Engineering, University of California, Berkeley, Berkeley, California (C-CP, NPF, CJR); Protea Biosciences Group, Morgantown, West Virginia (TR); and Vision Science Graduate Program, University of California, Berkeley, Berkeley, California (CJR).

Abstract

Purpose We developed an *in vitro* model-blink cell that reproduces the mechanism of *in vivo* fouling of soft contact lenses. In the model-blink cell, model tear lipid directly contacts the lens surface after forced aqueous rupture, mirroring the pre-lens tear-film breakup during interblink.

Methods Soft contact lenses are attached to a Teflon holder and immersed in artificial tear solution with protein, salts, and mucins. Artificial tear-lipid solution is spread over the air/tear interface as a duplex lipid layer. The aqueous tear film is periodically ruptured and reformed by withdrawing and reinjecting tear solution into the cell, mimicking the blink-rupture process. Fouled deposits appear on the lenses after cycling, and their compositions and spatial distributions are subsequently analyzed by optical microscopy, laser ablation electrospray ionization mass spectrometry, and two-photon fluorescence confocal scanning laser microscopy.

Results Discrete deposit (white) spots with an average size of 20 to 300 μm are observed on the studied lenses, confirming what is seen *in vivo* and validating the *in vitro* model-blink cell. Targeted lipids (cholesterol) and proteins (albumin from bovine serum) are identified in the discrete surface deposits. Both lipid and protein occur simultaneously in the surface deposits and overlap with the white spots observed by optical microscopy. Additionally, lipid and protein penetrate into the bulk of tested silicone-hydrogel lenses, likely attributed to the bicontinuous microstructure of oleophilic silicone and hydrophilic polymer phases of the lens.

Conclusions *In vitro* spoilation of soft contact lenses is successfully achieved by the model-blink cell confirming the tear rupture/deposition mechanism of lens fouling. The model-blink cell provides a reliable laboratory tool for screening new antifouling lens materials, surface coatings, and care solutions.

Key Words: contact lens, spread lipid, protein, tear-film rupture, deposition fouling

Comfort is a significant impediment to soft contact lens (SCL) wear, especially at end of day.^{1,2} When on the eye, an SCL is continually exposed to tear components including mucins, proteins, salts, and tear-film lipids. These

species interact with the lens to initiate “fouling.”³⁻⁷ Lens fouling or spoilation is generally classified into hazy films and discrete spot deposits.³⁻⁶ If thick enough, surface films can interfere with vision. The discrete spot deposits, generally referred to as “white spots”^{8,9} or “jelly bumps,”¹⁰ are elevated macroscopic patches consisting of lipids, proteins, inorganic salts, and possibly bacteria.^{8,9} Observed white spots can be tens of micrometers in size or even larger.^{8,9} In addition to interference with vision, the upper lid may experience physical irritation during blinking, further compromising comfort.^{1,2} Moreover, modern silicone-hydrogel (SiHy) materials are more hydrophobic than their conventional poly-hydroxyethyl methacrylate (pHEMA) ancestors. Accordingly, some studies indicate a tendency of SiHy lenses to accumulate more surface lipids, depending on the method of analysis.^{3,6,11-13} Understanding the etiology of white spots on SCLs remains a compelling topic for improved lens design.^{14,15}

Studies of lens spoilation and deposition are divided into two types: *ex vivo*^{3,6,8-10,16-24} and *in vitro*.^{6,11-13,20,23-34} In *ex vivo* studies, subjects wear lenses for a prescribed period. Worn lenses are then removed and analyzed for their lipid and protein content and composition. Although *ex vivo* studies are the gold standard for assessing lens fouling and are critical for any commercial product, they have major drawbacks. First, to overcome unavoidable variations in human behavior, a large subject sample size must be gathered for *ex vivo* experiments, which is labor intensive and time consuming. Second, there are many hidden variables in *ex vivo* studies that potentially affect the lipid/protein deposition, such as tear- and lipid-production rates and composition, lifestyle, and diet habit, in addition to uncontrolled roles of humidity and contamination by lens handling.³⁵ Third, it is nearly impossible to examine one study variable on lens physics and chemistry. Other variables including lens thickness and shape, edge design, bulk material, surface treatment, care/package solution, and so on are difficult to control in *ex vivo* studies. Most importantly, lipid chemical analysis is delicate with different research groups generating contrasting results for both composition and amount of lipid deposited.^{6,7,12} These issues lead to inconclusive results on how SCL chemistry influences lipid/protein deposition.¹⁴ *Ex vivo* studies are not suitable to screen expeditiously for new antifouling lens compositions and coatings during lens development.

For these reasons, a large number of *in vitro* spoilation studies have been performed on targeted molecules^{6,11-13,20,23-34} with the advantage of improved control and better reproducibility. Ideal *in vitro* spoilation studies require a representative “tear film” and a physically valid deposition mechanism. In most *in vitro* efforts, lenses are soaked in aqueous-dispersed lipids and proteins for a set time. Because tear proteins are aqueous soluble, this procedure is reasonable for assessing lens protein spoilation, but it is not so for lipids because most tear lipids, especially those that are nonpolar, are highly insoluble in water.^{10,36} Two avenues to overcome the solubility limitation are (1) to dissolve the lipid into an organic solvent, such as

chloroform/methanol, or (2) to disperse a lipid/solvent mixture into a cloudy emulsion of lipid droplets. Neither methodology occurs during lens on-eye wear. Correlation between *in vitro* and *ex vivo* spoiling studies is, thus, not expected.^{7,14,15,20} To bypass these obstacles but still maintain the advantages of *in vitro* screening for lens fouling, an *in vitro* fouling process must duplicate the SCL on-eye-wear deposition mechanism(s) and environment.

Hart et al.¹⁰ were apparently the first to describe a realistic mechanism for lipid deposition onto contact-lens surfaces. Rather than adsorb from the aqueous solution, free lipids initially spread on the tear film deposit directly onto the lens in “dry” spots where the tear film experiences breakage. Port⁴ summarizes the mechanism as “collapse of the overlying tear film when a ‘dry spot’ occurs on the lens surface.” Upon repeated blinking and tear rupture, a repetitive cascade of deposition events builds lipid mounds on the surface.

More recently, Copley et al.³⁷ describe the *in vivo* lens-fouling process as follows. After the pre-lens tear film is deposited during lid rise and the lens centers, evaporation reduces the pre-lens tear film thickness, making it vulnerable to rupture. Upon local rupture, the insoluble tear-film lipid layer comes into direct contact with the contact-lens anterior surface. Some lipid transfers to the lens surface and adheres. Lipid is “deposited,” not adsorbed from solution. The driving force for deposition is mechanical. Thus, the composition of the lipid on the contact lens is very similar to that of meibum in the lipid layer.¹⁰ When a new tear film is deposited, the oily remnant remains on the lens surface, making tear rupture and additional lipid deposition more likely in that region. In this manner, lipid patches build, and as they do, aqueous-soluble species may incorporate, such as protein and salt. The picture of Copley et al.³⁷ is consonant with the lipid-deposition process of Hart et al. and explains essentially all observed behaviors of how lens white spots form and grow.^{3-6,8-10}

Earlier attempts to replicate the lipid-deposition mechanism *in vitro* used a rocking-bed design^{32,38,39} that is unlikely to reflect tear breakup faithfully. More recently, Lorentz et al.²⁶ designed a model-blink-cell piston that cycles sample lenses in and out of artificial tear solution (ATS) containing dissolved trace amounts of radioactive ¹⁴C-cholesterol or ¹⁴C-phosphatidylcholine below their aqueous solubilities. There was no separate free lipid phase as there is during on-eye lens fouling. Here, too, it is doubtful that the resulting fouled lenses faithfully duplicate lipid deposits observed in *ex vivo* studies.

The aim of this study is to develop an *in vitro* model-blink cell that mimics the physical mechanism(s) of *in vivo* fouling of SCL surfaces. To achieve this goal, the model-blink cell need not replicate the entire tear-blink dynamics. Rather, it must capture the physical mechanism(s) of on-eye lens fouling. Following the original work of Copley et al.,³⁷ our model-blink cell deposits lipid onto SCLs, reproducing that actually occurring during on-eye wear.

METHODS

Soft Contact Lenses

Five commercial SiHy SCLs were used in this study, including ACUVUE ADVANCE (galyfilcon A) from VISTAKON (Jacksonville, FL), NIGHT&DAY (lotrafilcon A) and O₂OPTIX (lotrafilcon B) from CIBA VISION Corp (Duluth, GA), PureVision (balafilcon A) from Bausch + Lomb Inc (Rochester, NY), and Biofinity (comfilcon A) from CooperVision (Scottsville, NY). For comparison to the SiHy lenses, a single pHEMA-based SCL, ACUVUE 2 (etafilcon A) from VISTAKON, was also used in this study. The diameter, base curve, and power of these SCLs ranged from 13.8 to 14.0 mm, from 8.6 to 8.7 mm, and from -2.0 to -3.0, respectively. Each lens was soaked in excess amount of phosphate-buffered saline (PBS, pH = 7.4) for 48 hours before each experiment to remove preservatives and surfactants from the package solution.

Preparation of ATS and Artificial Tear-Lipid Solution

A pH 7.4 PBS solution was prepared as described earlier⁴⁰ and used as the base of the aqueous-phase ATS. If not stated, ATS in this study was composed of specific proteins, including lysozyme from egg white (3.28 mg/mL), β -lactoglobulin (1.25 mg/mL), mucin from bovine (0.035 mg/mL), and albumin from bovine (0.175 mg/mL) in PBS. All chemicals were acquired through Sigma-Aldrich (St. Louis, MO). Preparation of ATS was accomplished at most 24 hours before fouling experiment and stored at 4°C to prevent degradation.

The artificial tear-lipid solution (ATLS) was composed of selective polar and nonpolar lipids, including cholesterol (0.068 mg/mL), cholesteryl stearate (0.024 mg/mL), sphingomyelin (0.004 mg/mL), galactocerebrosides (0.004 mg/mL), and l- α -phosphatidycholine (0.004 mg/mL) in toluene. All chemicals were purchased from Sigma-Aldrich. After preparation, the tear-lipid solution was stored at -20°C for at most 1 month.

Blink-Cell Construction and Operation

Fig. 1 illustrates the concept underlying the model-blink cell. The posterior surface of an SCL is attached to a Teflon mold and immersed in ATS. Artificial tear-lipid solution is then spread over the air/ATS interface to form a duplex lipid layer.⁴¹ On the eye, tear-film lipid is renewed after each blink so lipid supply is continuous. Thus, as long as the ATLS is not depleted from the air/ATS interface, exact control of lipid-layer thickness is not requisite. Similar reasoning dictates that the exact volume of ATS in the model-blink cell is irrelevant to the deposition mechanism and can be chosen for convenience.

As illustrated in Fig. 1, ATS is slowly withdrawn from the exit port; the ATS level falls to drape over the contact lens. The draped aqueous film between the lipid layer and the contact lens ruptures. The expanding ATS rupture spots leave behind lipid, some of which “deposits” directly onto the lens surface. Subsequently, ATS is injected to reestablish the aqueous layer

between the lens and lipid film at the air/water interface, as shown in Fig. 1. The steps in Fig. 1 replicate the mechanical process that deposits lipid onto the anterior surface of contact lenses. Each blink event in the model-blink cell guarantees tear rupture. Consequently, establishing a 5-second blink cycle is unnecessary. Cycle time can be chosen for experimental convenience. Finally, an SCL after centering on eye is static during the interblink when tear rupture occurs. Replication of lens motion during the blink is, thus, not pertinent to the deposition mechanism. The post-lens tear film does not participate in tear rupture and, hence, is not a source of lipid contamination. We assert that the model-blink cell in Fig. 1 faithfully reproduces the actual tear-rupture/lipid deposition mechanism of SCL fouling.

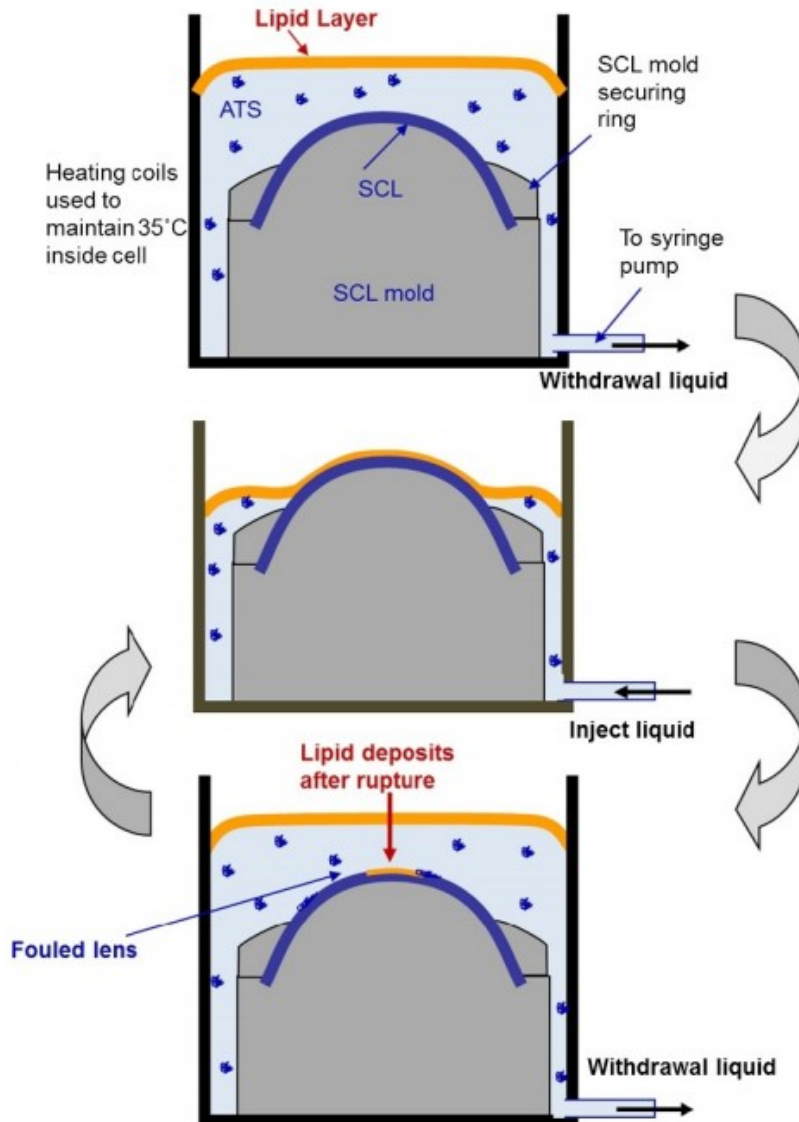


FIGURE 1.

Schematic representation of *in vitro* lipid deposition on an SCL in the model-blink cell. A color version of this figure is available online at www.optvissci.com.

Fig. 2 shows the custom-built model-blink cell modified from that of Copley et al.³⁷ Inner walls of the Plexiglas cell are covered with a removable customized-glass lining to prevent lipid wall accumulation during the fouling experiment. A programmable precision microsyringe pump (SYR-1200, J-KEM Scientific, St. Louis, MO) controlled by an in-house written program (Labview 7.0, National Instruments, Austin, TX) injects and withdraws aqueous solution into and out of the cell to duplicate the tear-film thickness change during blinks. In addition, a copper-heating coil surrounds the cell to maintain the temperature at 35°C .

The tested SCL is attached to a two-piece Teflon holder with an 11.2-mm-diameter circular opening to expose a controlled area of the anterior lens surface to the ATS. The holder is subsequently screwed into the model-blink

cell to fix its position, as shown in Fig. 2. For a typical run, 6 mL of ATS is pumped into the cell to immerse the lens holder, and 200 μ L of tear-lipid solution is spread onto the solution surface to form a tear-film lipid layer. The system is left undisturbed for 20 minutes to allow evaporation of the tear lipid solvent (toluene) and temperature equilibration to 35°C. To ensure that toluene completely evaporates without significantly changing the volume of aqueous phase, a 5-cm-diameter electric fan (Sunon, Kaohsiung, Taiwan) is positioned 30 cm above the cell. For efficient solvent removal, the fan circulates air at a moderate speed (\sim 2500 rpm) toward the lipid/air interface. After about 20 minutes when solvent disappears, the fan is turned off and blink deposition is started. Three mL of ATS is slowly pumped out of the apparatus, which lowers the insoluble lipid layer into contact with exposed SCL anterior surface. Tear solution is then subsequently injected back into the apparatus to reform the aqueous layer between the lipid layer and the SCL, thereby completing the blink cycle. One complete cycle lasts 12 seconds, with the lipid layer in contact with the SCL for 6 seconds. After every 100 complete cycles, fresh lipid and protein solution replaces the used solutions to ensure that the lipids/protein in the cell are not depleted, and the cycling process is reinitiated after another solvent evaporation/temperature equilibrium waiting period. Unless otherwise noted, all lenses are exposed to a total of 300 cycles. The chosen cycle number reflects about 300 on-eye blinks with tear rupture and gives sufficient deposition for ease of viewing and analysis. After cycling, the contact lens is detached from the cell and lightly rinsed with PBS to remove loosely bound lipids and proteins. The lens sample is then stored in fresh PBS for subsequent examination, including deposit morphology, lipid deposit amount, and lipid and protein composition and distribution.

Deposit Morphology

Morphology of the deposits on the surface of fouled lens was obtained with an optical microscope (Olympus BX51, Tokyo, Japan) attached to a color digital camera (Olympus C-5060, Tokyo, Japan). The fouled lens remained hydrated in PBS during measurement.

Lipid Extraction from Fouled Lenses

The *in vitro* fouled lens was rinsed with deionized water and immersed in a glass vial containing 4 mL of toluene/isopropanol (EMD Chemicals, Philadelphia, PA) solution (5:1 in volume ratio). To extract lipid from the fouled lens, the sample vial was immediately sonicated at 42 kHz in a water bath with an ultrasonic cleaner (Cole Parmer, Vernon Hills, IL) at room temperature for 15 minutes. Extracted lipid solution was removed into a clean 7-mL glass vial and placed in a vacuum chamber overnight to remove solvent. Once the solvent was completely evaporated, the sample was sealed and kept at -20°C before examination for lipid mass. For each SCL, clean lenses were also studied by an identical procedure to correct for

nascent materials in the clean contact lens that might dissolve into the organic solvent.

To determine the mass of lens-extracted lipid, 100 μL of chloroform (Fisher Scientific, Fair Lawn, NJ)/methanol (EMD Chemicals) solution (2:1 in volume ratio) was added to a pre-evacuated vial, followed by moderate vortexing to ensure that lipids completely dissolve. Subsequently, 1 to 3 μL of sample solution was evenly spread into a 45- mm^2 circle marked on the surface of a standard test-grade silicon wafer (475 to 575 μm in thickness, International Wafer Services, Colfax, CA). Once the solvent evaporated, the thickness profile of lipid deposition on the wafer was determined by ellipsometry (Sentech SE 400, Berlin, Germany) following procedures described by Maurer et al.⁴² To permit lipid-thickness calculation, the refractive index of the lipid deposit was set at 1.45.⁴³ Average lipid thickness was estimated from measurements on more than 100 points within the sample circle. Mass of lipid was calculated with an average density of lipids as 0.9 g/cm^3 .⁴¹ All solvents are HPLC grade (>99.9%) and are used without further purification.

Laser Ablation Electrospray Ionization Mass Spectrometry

Laser ablation electrospray ionization mass spectrometry (LAESI-MS; Protea Biosciences Group, Morgantown, WV) was used to construct two-dimensional (2-D) and three-dimensional (3-D) maps of selective molecules on and in fouled lenses. To increase signal sensitivity in the fouling experiments, only selective chemicals, lysozyme (9.41 mg/mL in PBS), mucin from bovine (0.035 mg/mL in PBS), and phosphatidycholine lipid (0.52 mg/mL in toluene), were included in the ATS and tear-lipid solution, respectively. ACUVUE ADVANCE was used in this study. After fouling in the model-blink cell, lenses were analyzed within 7 days using the Protea LAESI DP-1000 system connected to a Thermo LTQ Velos mass spectrometer. For 2-D mapping, the lens was ablated with 20 laser pulses at 10 Hz at each location, and for the 3-D profiling, a frequency of 1 Hz was used for laser 40 pulses to allow the mass spectrometer sufficient time to collect data for each pulse. A spatial resolution of 360 μm was used for the 2-D mapping and 200 μm was used for depth profiling. The mass spectrometer was operated in positive-ion mode using an electrospray solution of 0.1% aqueous acetic acid solution in 50% methanol. The electrospray solution was introduced at 1 $\mu\text{L}/\text{min}$ with an electrospray voltage of 4 kV. Each lens analyzed was first rinsed in deionized water, placed on a glass slide, and sliced radially near the periphery to ensure that the contact lens laid flat on the microscope slide. After loading into the instrument, the sample stage was kept at -10°C to prevent lens drying during analysis. The mass spectrometer acquired data over a mass range from 100 to 2000 m/z . After data acquisition, data files were imported in ProteaPlot software to generate ion maps for the selected molecules.

Fluorescence Confocal Scanning Laser Microscopy

Two-photon fluorescence confocal scanning laser microscopy (FCSLM) determined the composition of the labeled materials in spot deposits on the

in vitro fouled lens surface via a Carl Zeiss 510 LSM META NLO AxioImager confocal microscope (Carl Zeiss GmbH, Jena, Germany). The ATS was prepared as described in Preparation of ATS and Artificial Tear-Lipid Solution with an additional 62.5 µg/mL of bovine serum albumin (BSA) labeled with Alexa Fluor 488 conjugate (Life Technologies, Grand Island, NY). Lipid concentration was five times higher than that of typical ATLS in the study described earlier. Additionally, to stain lipid deposits on the SCL surface, 200 µg/mL of Nile Red (Life Technologies) was mixed into the lipid solution before the spoilation experiment. Alexa Fluor-conjugated BSA from the fouled lens was detected with excitation at 488 nm from an argon laser and emission through a 500- to 530-nm band-pass filter. Nile Red-stained lipids were observed with excitation at 543 nm from a HeNe laser and emission through a 650- to 710-nm band-pass filter. Control experiments were conducted to ensure that the two excitation-emission spectra did not overlap, thereby allowing separate signals from BSA and lipids.

We also used two-photon FCSLM to follow penetration profiles of tagged lipids³² similar to earlier work.⁴⁰ The ATS and ATLS were prepared as described in Preparation of ATS and Artificial Tear-Lipid Solution, except that cholesterol was replaced with fluorescently tagged 25-[N-[(7-nitro-2-1,3-benzoxadiazol-4-yl)methyl]amino]-27-norcholesterol (25-NBD cholesterol; Avanti Polar Lipids, Alabaster, AL). Fluorescence emission was collected with a Plan-Neofluar 10×/0.30 NA objective (Carl Zeiss GmbH) using a 500- to 550-nm emission filter.

RESULTS

Surface Analysis of Fouled SCLs

Fig. 3 shows optical micrographs at three different magnifications of the surface of a fouled ACUVUE ADVANCE after 300 cycles in the model-blink cell. Random deposits are evident on the surface with sizes ranging from 30 to 200 µm. These results confirm that our *in vitro* model-blink cell successfully forms lens deposits with similar morphology to those observed on SCLs worn on eye.^{8,9} Size and number of these deposit spots are controlled by the number of cycles to which the lens is subjected. After 300 cycles of the model-blink cell, mound deposits are clearly visible to the naked eye.

Fig. 4 shows micrographs from the two-photon FCSLM examination of lipid deposition on the surface of two different fouled SiHy SCLs. After replacing lipid cholesterol with fluorescently tagged cholesterol, lipid deposits are reflected by bright yellow-green spots with equivalent patterns on both lens surfaces after 300 cycles. The lipid deposits display patterns similar to the white spots observed by optical microscopy on the fouled lenses. For a PHEMA-based SCL, however, no specific bright spots were found on the surface after the identical 300-cycle treatment in the model-blink cell (image not shown).

To study the role of both protein (lysozyme) and lipid (phosphatidycholine) in the spoilage of SCLs, LAESI-MS was used to establish a 2-D mapping on the surface of a fouled ACUVUE ADVANCE. Fig. 5 reveals both lysozyme and phosphatidycholine in the mound deposits on the surface of the lens. After filtering the signal of desired molecule from the background of polymer fragments taken from a nascent lens, randomly distributed discrete spots (shown as colored spots) of lysozyme (Fig. 5A) and phosphatidycholine (Fig. 5B) are seen on the lens surface. Ion mapping from LAESI-MS was overlaid on an optical image to demonstrate that the colored spots containing lysozyme in Fig. 5A coincide with optically observed deposit spots on the lens, as demonstrated in Fig. 6. Dark regions of the optical image correspond to the deposit spots where the deposition on the surface protects the SCL polymer matrix from damage by the applied laser. Fig. 6 shows that the contours of the ion map correspond to the lysozyme deposits. It is clear that lysozyme deposition overlaps with the optically seen deposit bumps on the surface. A similar result was also observed for phosphatidycholine lipid in the surface deposit (data not shown). Surface-imaging patterns for lipids and proteins from both FCSLM and LAESI-MS correspond to each “white” deposit spot on the contact-lens surface.

It is imperative to inquire whether lipid and protein occur simultaneously in the same deposits. Fig. 7 shows two-photon FCSLM images of deposit spots garnered at different emission wavelength on fouled ACUVUE ADVANCE surface. Both protein (BSA) and lipid (stained with Nile Red) were detected in the identical optical deposit spots, confirming that the deposit spots generated in the model-blink cell contain the selected lipid and protein together. We find, however, that protein and lipid distributions are not uniform within the same deposit. Some very bright spots of Alexa Fluor-conjugated BSA were detected inside deposit spots where the intensity from Nile Red-stained lipid is relatively uniform. Although deposit spots contain the selected lipid and protein simultaneously, they apparently do not do so in the same relative amounts.

Depth Profiling of Proteins and Lipids in SCLs

In addition to surface scanning, FCSLM and LAESI-MS allow depth profiling of targeted molecules in the bulk lenses fouled in the model-blink cell. Fig. 8 shows depth-scanning profiles of 25-NBD cholesterol by two-photon FCSLM. Profiles were measured at 12 and 100 hours after fouling. At 12 hours (Fig. 8A, B), the fluorescence intensity is locally concentrated toward the top (anterior) surface for both SiHy lenses. This increased intensity corresponds to the lipid deposits on the surface of the fouled lenses. In Fig. 8C, D, after the fouled lenses were stored for 100 hours in fresh PBS solution (in which lipid solubility is negligible), surface lipids gradually penetrated into the lens. Measured profiles in Fig. 8C, D are more intense near the original surface deposit but now are dispersed throughout the bulk of the lens. For the pHEMA-based ACUVUE 2, however, no penetration of lipid is observable within the sensitivity of FCSLM (data not shown).

Fig. 9 shows comparable depth profiles of lysozyme protein and phosphatidylcholine lipid from LAESI-MS for a model-blink-cell fouled ACUVUE ADVANCE lens. Lysozyme is observed throughout the lens (Fig. 9A) as shown by the observed contours in each pulse. The amount of detected molecules is represented by the color index where red represents higher concentration whereas blue indicates lower concentration. The majority of phosphatidylcholine was detected on the surface of contact lens (Fig. 9B). Interestingly, the highest concentration of lysozyme is evident in the middle of the fouled lens. This result indicates that lysozyme penetrates into the SiHy SCL during the fouling process. Because only the anterior surface of SCLs is in direct contact with the aqueous lysozyme solution in the model-blink cell, lysozyme concentration should be higher in the anterior region of the lens than that in the posterior region. However, after the spoilation process, the fouled lens was stored in fresh PBS for 5 days, allowing lysozyme to leach from the fouled lens into the surrounding PBS. Leaching causes the decline in lysozyme concentration seen in Fig. 9A near the anterior lens surface. This result suggests that lysozyme uptake/adsorption rate by the SCL matrix is much faster than the release/desorption rate. Phosphatidylcholine penetration from surface deposit into the bulk of the lens is shown in Fig. 9B. It is, however, not as significant compared with that observed from two-photon FCSLM for fluorescent-tagged cholesterol.

Lipid Extraction from Fouled Lenses

Total lipids extracted per lens from various fouled lenses are shown in Fig. 10. The amount of lipid extracted includes lipid uptake by the bulk contact lens in addition to that by the anterior surface. Among the six commercial SCLs studied, silicone-based ACUVUE ADVANCE exhibits the highest amount of lipid ($10.22 \pm 1.08 \mu\text{g}$), whereas pHEMA-based ACUVUE 2 demonstrates the lowest amount ($2.39 \pm 1.06 \mu\text{g}$). All five SiHy SCLs exhibit higher amounts of lipid extracted compared with that of the pHEMA-based ACUVUE 2 lens. Based on the observations from both FCSLM and LAESI-MS (Figs. 8 and 9), however, lipid penetration into the bulk of lens materials is negligible compared with that for surface deposition during the *in vitro* fouling process in the model-blink cell. Accordingly, the results in Fig. 10 give the amount of lipid deposited on the fouled lens surface. Further, lenses were stored in fresh PBS after fouling, allowing time for lipids on the surface to rearrange and to penetrate gradually into the bulk of SCL hydrogel matrix. Extraction measures all lipid present on or in the lens; thus, the total amount extracted reflects that deposited onto the lens surface during exposure to ATLS in the blink cell.

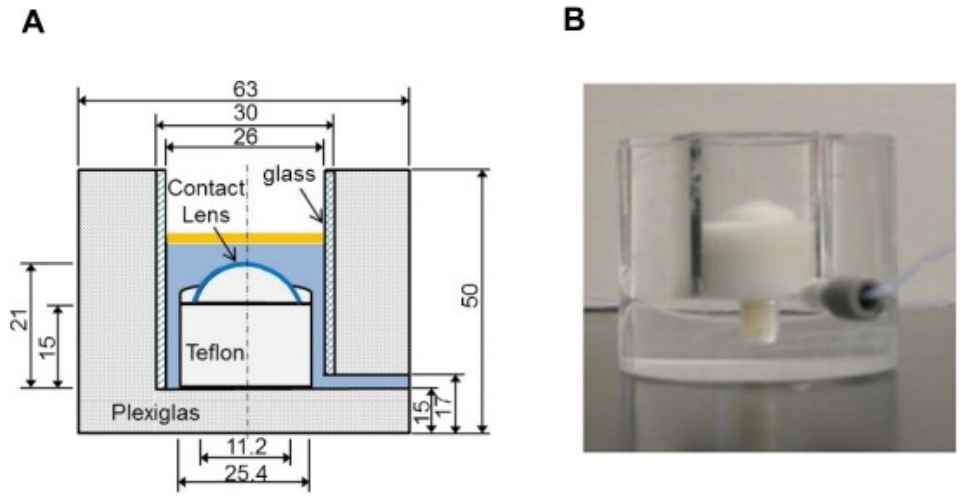


FIGURE 2. (A) Schematic and (B) photograph of the *in vitro* model-blink cell. Dimensions of design are in millimeters. Figure is not drawn to scale. A color version of this figure is available online at www.optvissci.com.

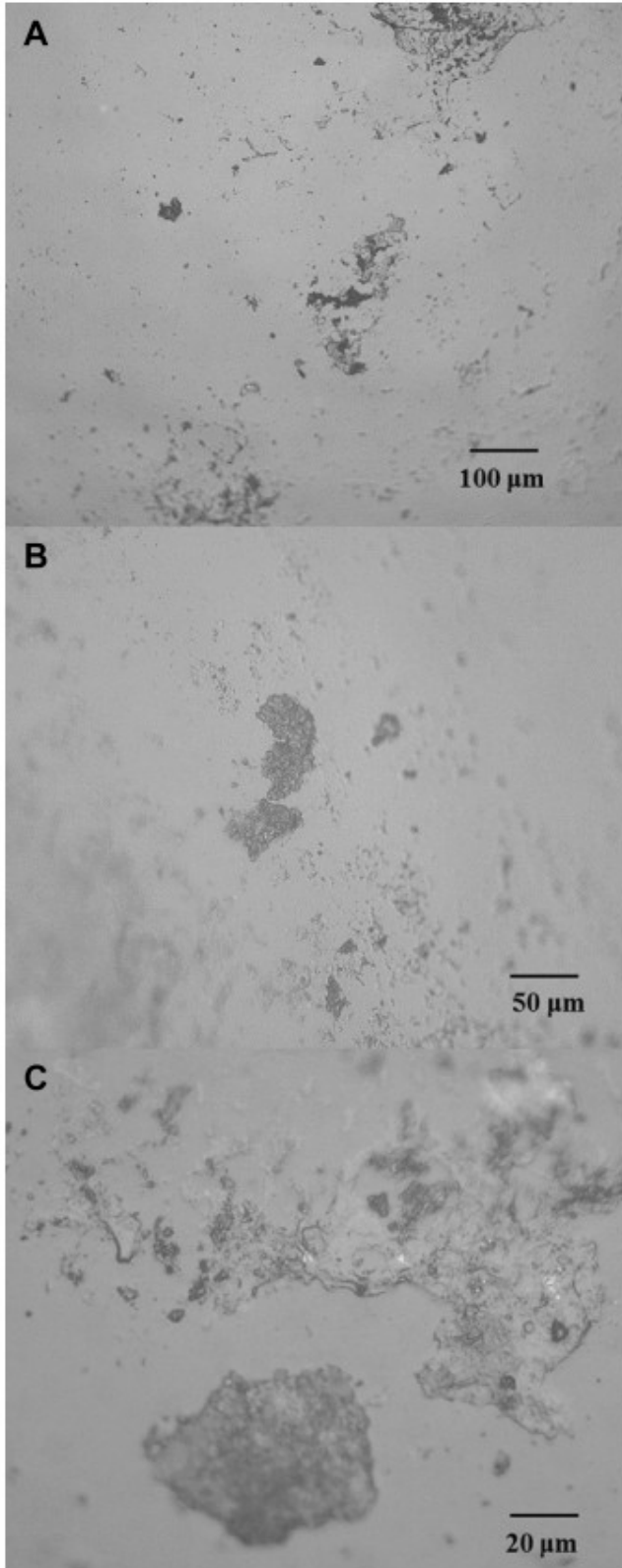


FIGURE 3. Random deposit spots on the surface of fouled lens (ACUVUE ADVANCE) after 300 blink cycles. (A) 10×, (B) 20×, (C) 50×.

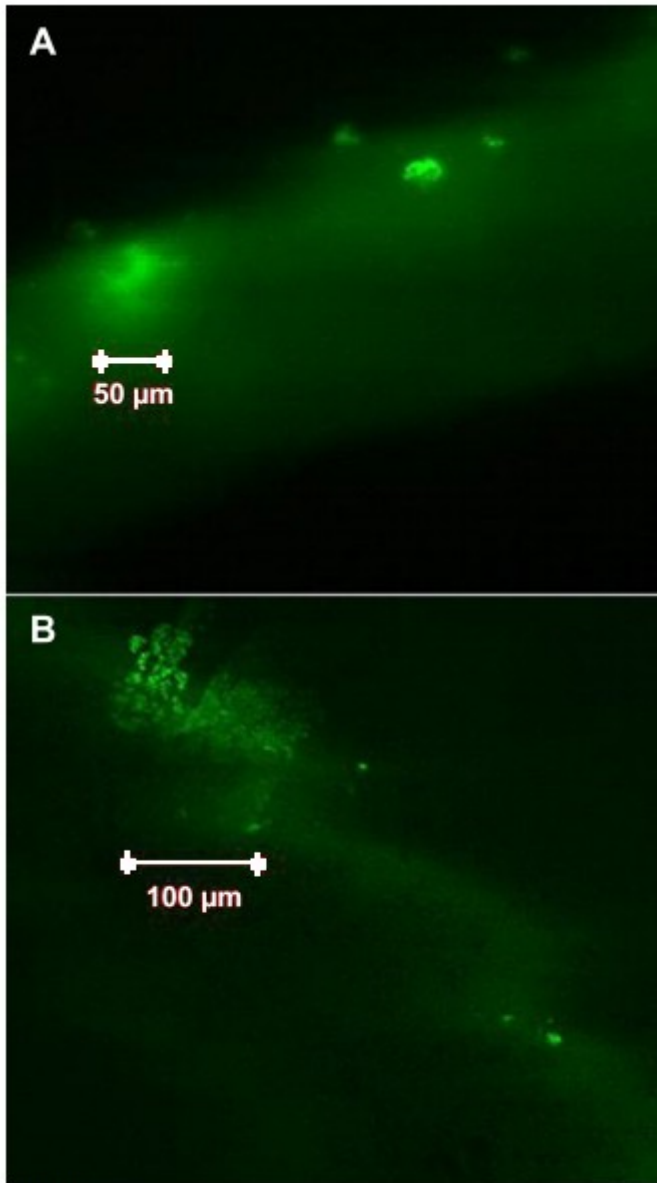


FIGURE 4. Discrete lipid (25-NBD cholesterol) deposition spots from fouled SiHy contact lenses (A) ACUVUE ADVANCE and (B) NIGHT&DAY by two-photon FCSLM. A color version of this figure is available online at www.optvissci.com.

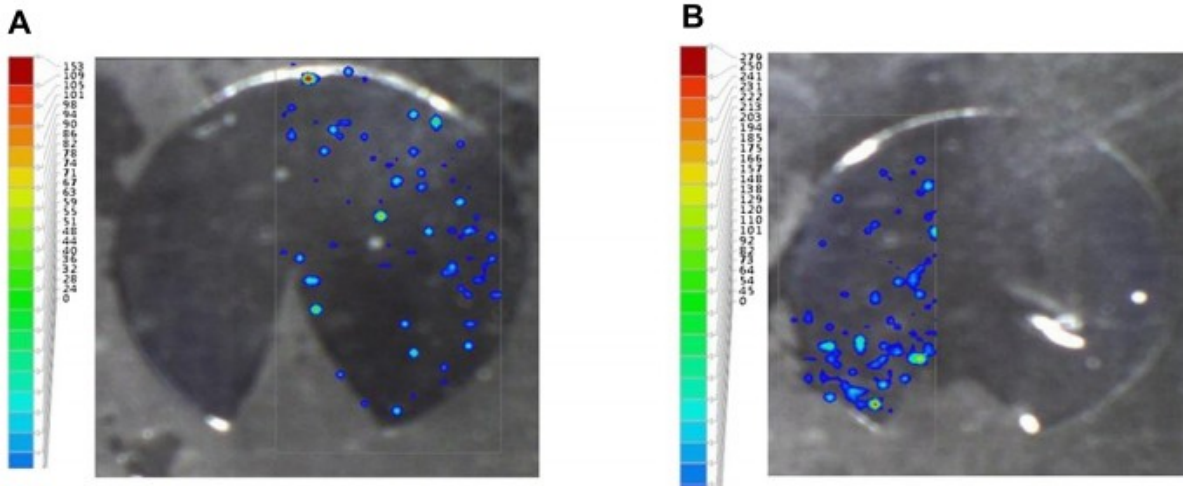


FIGURE 5. Two-dimensional ion maps of contact lens (ACUVUE ADVANCE) showing distribution of (A) lysozyme charged state m/z 1590.7 and (B) phosphatidylcholine lipid m/z 760.8 after 300 cycles in the model-blink cell. Numbers adjacent to color bar represent relative intensities in a.u. A color version of this figure is available online at www.optvissci.com.

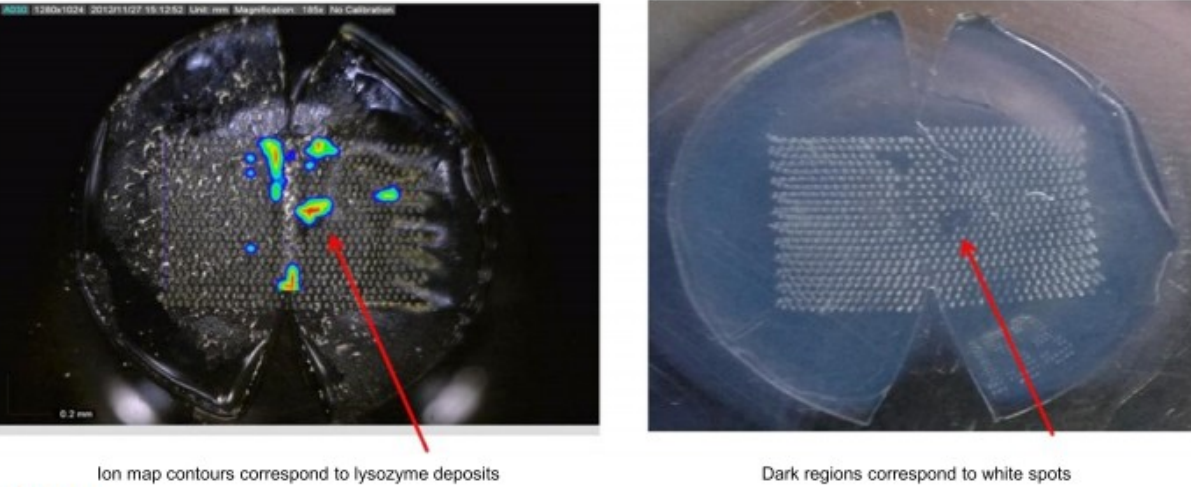


FIGURE 6. Ion map of lysozyme from LAESI-MS (left) overlaid on optical image (right) of fouled ACUVUE ADVANCE. The dark region on the right corresponds to the bright region on the left. A color version of this figure is available online at www.optvissci.com.

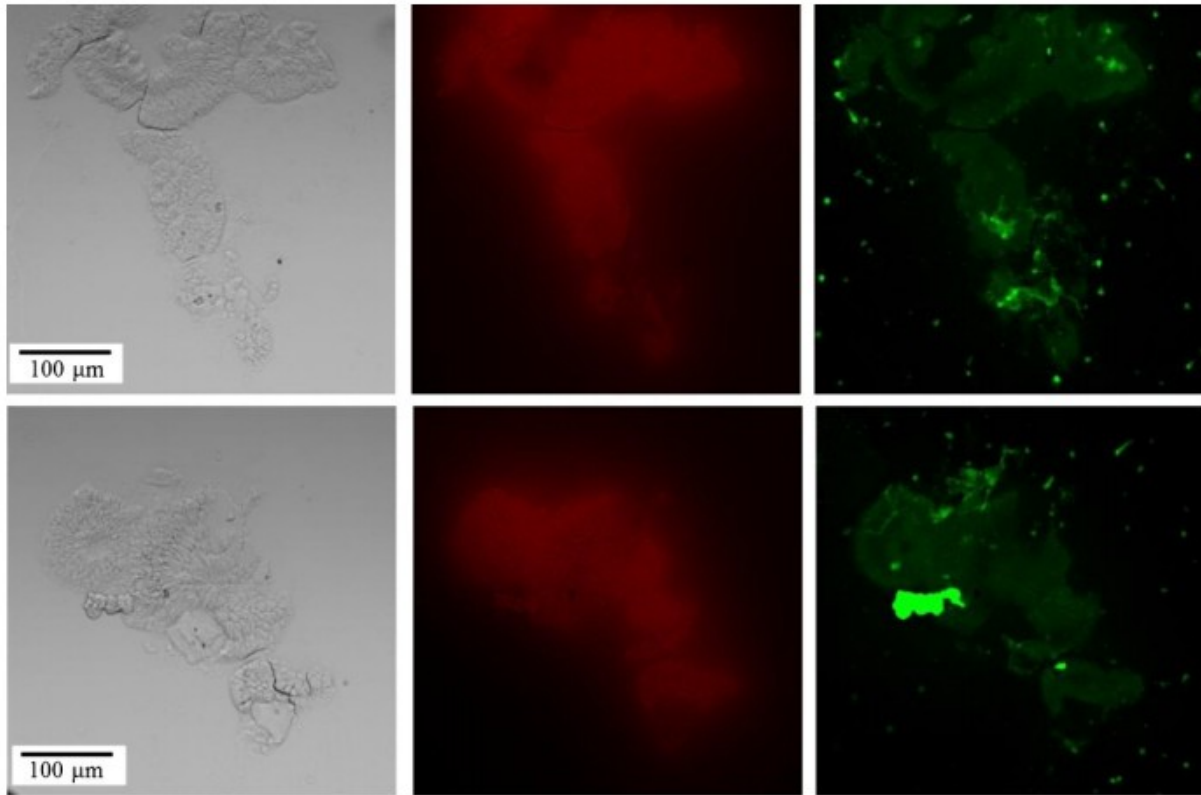


FIGURE 7.

Discrete deposition spots from ACUVUE ADVANCE fouled in the model-blink cell by two-photon FCSLM. Left, optical image; middle, Nile Red-stained lipids; right, Alexa Fluor-conjugated BSA. Micrographs in each row were taken at the same optical spot. A color version of this figure is available online at www.optivisci.com.

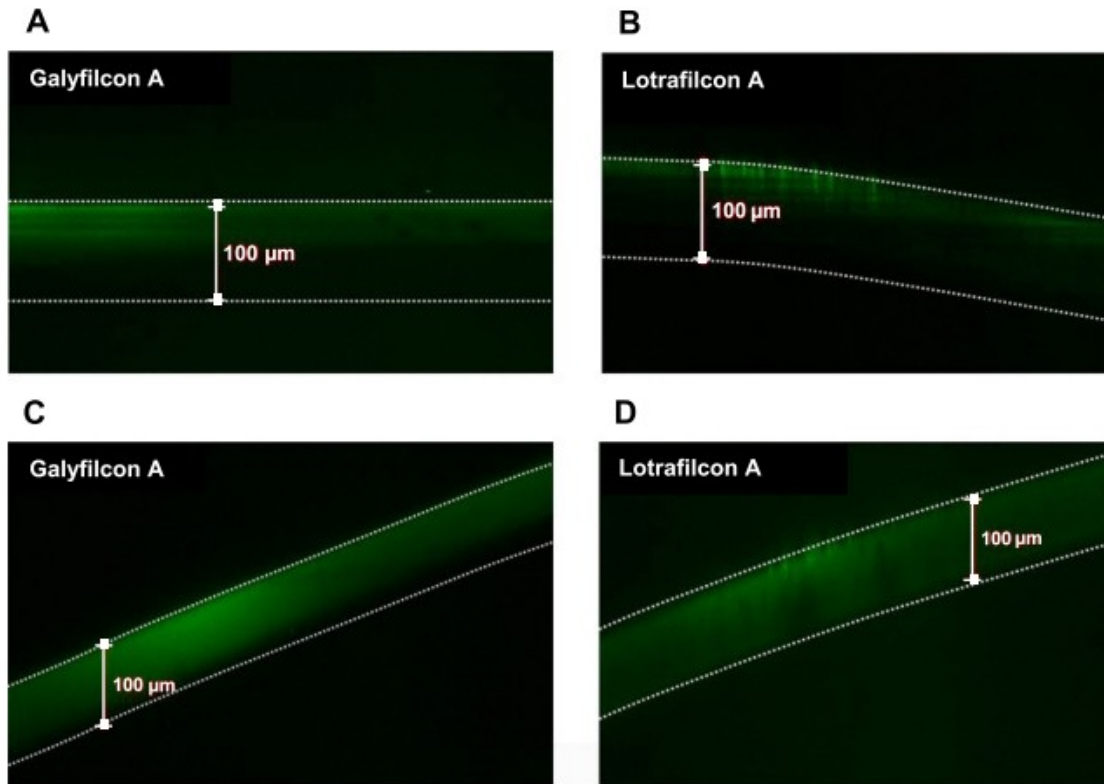


FIGURE 8.

Depth-scanning profiles of 25-NBD cholesterol in fouled SiHy SCL lenses by two-photon FCSLM. Observations were carried out 12 hours (A and B) and 100 hours (C and D) after lenses were fouled in the model-blink cell. A color version of this figure is available online at www.optvissci.com.

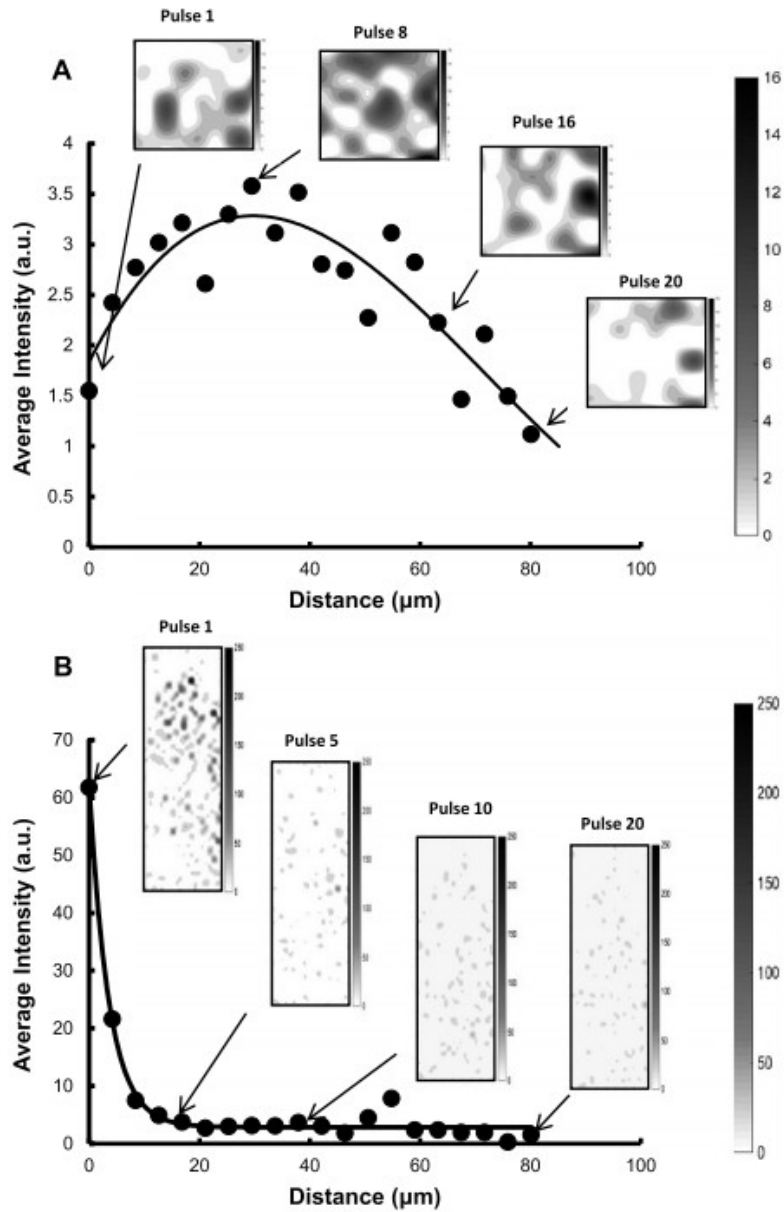


FIGURE 9.

Depth profiling of (A) lysozyme and (B) phosphatidylcholine lipid from *in vitro* fouled ACUVUE ADVANCE (300 cycles). Twenty laser pulses were used to profile through the lens. Separate 2.9 mm \times 2.9 mm and 7.9 mm \times 18.7 mm regions from the identical fouled lens were used for lysozyme and phosphatidylcholine, respectively. Solid lines provide visual guidance.

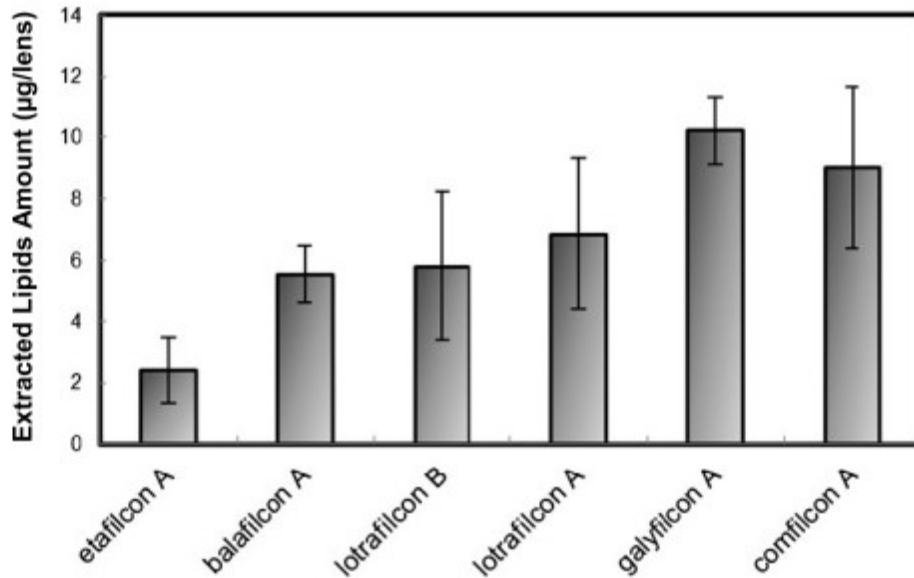


FIGURE 10.

Total extracted lipid amount from SCLs after 300 cycles. Data are presented as average \pm SD (n = 3).

DISCUSSION

It is not possible for insoluble tear-film lipid to transport by diffusion to the surfaces of an SCL. Shuttling of lipid through the tear film by oleophilic-decorated proteins (e.g., lipocalin) or unidentified micelles/vesicles is unproven, thermodynamically unfavorable, and must lead to uniform lens coatings rather than lipid mounds.^{37,44,45}

We developed an *in vitro* model-blink cell to “deposit” tear-film lipids onto SCLs by a physical mechanism representative of that encountered during on-eye wear. Microscopic analyses reveal randomly distributed deposits (i.e., white spots) on fouled SiHy SCL surfaces that contain simultaneously proteins and lipids. *In vitro* deposit spots were successfully created on SCL surfaces of similar size, composition, and distribution patterns to those from *ex vivo* observations.^{8,9} Incorporation of the actual tear breakup mechanism is critical to the success of an *in vitro* SCL-fouling model. Our model-blink cell provides a well-controlled environment that replicates tear-film rupture dynamics during blinking. Tear-film lipid is deposited onto the SCL, not adsorbed from aqueous solution.

The aim of our *in vitro* model-blink cell is to screen contact lenses for potential fouling consistent with the on-eye tear-rupture/lipid-deposition mechanism. Requirement for expensive and time-consuming *ex vivo* experiment is reduced. Our model-blink cell assesses *in vivo* fouling of SCL surfaces by mimicking the actual tear-rupture/lipid deposition mechanism. Replication of the entire human-blink process is not requisite. The chosen ATS volume (6 mL) and blink rate (every 12 seconds) for the model-blink cell need not reflect actual average *in vivo* values ($\sim 7 \mu\text{L}$, ~ 5 to 6 seconds).^{46,47}

We confirm that the proposed *in vitro* blink cell imitates the mechanism of on-eye lens fouling, as verified by multiple design experiments including random discrete deposit spots, spot size and size distribution, spot composition, and foulant lens penetration. Two major advantages of the model-blink cell are demonstrated. First, it is universal for various lipids/protein compositions as long as the tear-rupture/lipid-deposition fouling mechanism dominates. Second, identity and concentration of selected target molecules can be studied to elucidate the roles of specific tear components and their mixtures. Accordingly, the model-blink cell yields fundamental information on lipid-deposition amounts and kinetics on SCLs. We conclude that the model-blink cell provides a reliable screen for devising new antifouling lens materials, surface coatings, and care solutions.

For SiHy SCLs, random deposits were formed in all cases, demanding that the deposition process is mainly mechanical rather than chemical. When β -lactoglobulin, a lipocalin protein, was removed from the ATS, deposit spots still formed. This is direct proof against lipid deposition via aqueous protein delivery. Most spoilation studies focus on the total amount of lipid/protein deposited on the SCL whereas the effect of size and location distributions of these surface deposits is not explored. Many SCL-wear properties important to safety and comfort, such as wettability, surface roughness, friction coefficient, and bacterial adhesion/growth, depend not only on the total amount of deposits but also on the size and distribution of those deposits. This information is successfully replicated with our model-blink cell.

Although deposited lipid spots on the lens anterior surface have been intensively studied, as recently reviewed by Lorentz and Jones,⁶ understanding on whether and/or how lipid penetrates into hydrogel matrix is not conclusive because of the limitation of analysis techniques. Earlier studies indicated that lipids slightly penetrate into conventional hydrogel SCLs at the region below the surface lipid-deposit spots.^{10,48} Subsequently, a “push/pull” theory was developed to explain the difference of lipid deposition/absorption for various type of conventional hydrogel SCLs,^{28,48} in which the “pull” represents the adherence to the lens polymer strands and the “push” represents the water in the lens material driving insoluble lipid into the matrix. However, this process, if applicable, is extremely slow (up to a few months). Further, the amount of lipid that penetrates into the matrix of pHEMA-based lenses was negligible or not detectable compared with that in the deposits on the lens surface.^{10,18,49} For modern SiHy SCLs, however, the silicone copolymer dissolves organic material. If silicone microdomains in the lens are interconnected and continuous, dissolved lipid has a pathway through the lens. Studies of lipid penetration can then be a probe of microdomain structure in a contact lens. Jacob et al.³⁸ used Sudan IV³² and fluorescent-labeled cholesterol and phosphatidylcholine to observe the lipid penetration through SCLs. We adopt two-photon FCSLM to follow penetration profiles of tagged lipids on fouled lenses⁴⁰; our observations are consistent with those of Jacob et al. in that lipid penetration is significant in silicone-

based SCLs and undetectable in pHEMA-based SCLs. We observe lipid penetration subsequent to lens storage after fouling. This finding demands lipid diffusion/sorption into the gel matrix.

In addition to lipid penetration, we find from LAESI-MS that protein (lysozyme) penetrates into SiHy SCLs (ACUVUE ADVANCE). Protein deposition on contact lens surfaces has been intensively studied and recently reviewed by Luensmann and Jones.⁵⁰ Because lysozyme is positively charged at physiological pH, penetration assuredly occurs in the hydrophilic microdomains of a SiHy SCL. For ACUVUE ADVANCE lenses, simultaneous lipid and protein penetration into the bulk of the lens strongly suggests a bicontinuous microstructure of silicone and hydrophilic polymer microdomains in the lens. Significant amounts of lysozyme were detected from the model-blink-cell fouled lens (ACUVUE ADVANCE) exposed to aqueous protein solution for only 3 hours and subsequently stored in fresh PBS for 5 days. Thus, lysozyme uptake kinetics is much faster than release kinetics by SiHy SCLs, likely because of the strong adsorption on the polymer chains.^{51,52}

Quantitative analysis of lipid composition and amount on fouled lenses, either *ex vivo* or *in vitro*, is a major challenge because different analytic techniques and procedures yield differing sensitivity, accuracy, availability, and convenience. Literature reports different amounts and compositions of fouled deposits using different analytic instrumentation and extraction techniques.^{6,12,16,22,31} *Ex vivo* fouling is especially challenging as the number of components is large, difficult to identify, and not the same for each human subject. In our study, total lipid extraction ranges from 2.39 to 10.22 $\mu\text{g}/\text{lens}$, which is comparable to most reported *ex vivo* and *in vitro* studies.^{16,21,22,31} These studies require an on-eye wear or incubation period from a few days to as long as a month. In the model-blink cell, significant tear-film breakup occurs upon each blink, which is not likely during on-eye contact-lens wear. Our experiment protocols can be accomplished in a few hours providing a fast approach for assessment of lens fouling.

ACUVUE ADVANCE lenses demonstrated the highest amount of total lipid deposition after 300 cycles in the model-blink cell. Although the difference of lipid-deposition amounts for the various SiHy SCLs was not statistically significant (because of limited trials), our results clearly show that PBS-extracted SiHy SCLs exhibit higher total lipid deposition compared with pHEMA-based SCL (ACUVUE 2). Our findings are consistent with the general conclusion from previous studies for lipid deposition on SCLs both *ex vivo* and *in vitro*.^{22,26,31-33,53} We establish that both lipid and protein are present simultaneously in the white-spot deposits. Because of limited instrument sensitivity, however, we are unable to assess the sequence of lipids and proteins in the deposits.

CONCLUSIONS

An *in vitro* model-blink cell that forms lipid deposits on SiHy contact-lens surfaces, consistent with those observed during on-eye lens spoilation, was developed. Randomly distributed mound deposits containing both proteins and lipids are confirmed. Likewise, both lipid and protein penetrate into the bulk of SiHy SCLs, most likely because of a bicontinuous microstructure of these lenses. In addition to various SCLs, specific model lipids and tear solutions can readily be studied. The model-blink cell provides a reliable screen for future assessment for antifouling lens materials, surface coatings, and care solutions.

Clayton J. Radke

Department of Chemical and Biomolecular Engineering

University of California, Berkeley

101E Gilman Hall

Berkeley, CA 94720-1462

e-mail: radke@berkeley.edu

ACKNOWLEDGMENTS

This work was partially funded by Alcon Corporation under Contract 030046-005 to the University of California. We thank Colin Cerretani for discussion, Rachel Segalman for use of the optical microscope, Tatiana Svitova for the design of the lipid-extraction experiment, and David Liu for conducting FCSLM.

REFERENCES

1. Fonn D. Targeting contact lens induced dryness and discomfort: what properties will make lenses more comfortable. *Optom Vis Sci* 2007; 84: 279-85.
2. Nichols JJ, Sinnott LT. Tear film, contact lens, and patient-related factors associated with contact lens-related dry eye. *Invest Ophthalmol Vis Sci* 2006; 47: 1319-28.
3. Jones L, Senchyna M, Glasier MA, Schickler J, Forbes I, Louie D, May C. Lysozyme and lipid deposition on silicone hydrogel contact lens materials. *Eye Contact Lens* 2003; 29: S75-9.
4. Port MJA. Contact lens surface properties and interactions. *Optom Today* 1999; 39: 27-35.
5. Tighe BJ. Contact lens materials. In: Phillips AJ, Speedwell L, eds. *Contact Lenses*, 4th ed. Oxford, UK: Butterworth-Heinemann; 1997: 50-92.
6. Lorentz H, Jones L. Lipid deposition on hydrogel contact lenses: how history can help us today. *Optom Vis Sci* 2007; 84: 286-95.
7. Nichols JJ. Deposition on silicone hydrogel lenses. *Eye Contact Lens* 2013; 39: 20-3.

8. Bowers RW, Tighe BJ. Studies of the ocular compatibility of hydrogels. White spot deposits—chemical composition and geological arrangement of components. *Biomaterials* 1987; 8: 172-6.
9. Bowers RW, Tighe BJ. Studies of the ocular compatibility of hydrogels. White spot deposits—incidence of occurrence, location and gross morphology. *Biomaterials* 1987; 8: 89-93.
10. Hart DE, Tidsale RR, Sack RA. Origin and composition of lipid deposits on soft contact lenses. *Ophthalmology* 1986; 93: 495-503.
11. Panthi S, Hanlon SD, Burns AR, Nichols JJ. Delta Vision Spectris imaging of lipid deposits on contact lens surfaces. *Invest Ophthalmol Vis Sci* 2014; 55:E-abstract 6060.
12. Maziarz EP, Stachowski MJ, Liu XM, Mosack L, Davis A, Musante C, Heckathorn D. Lipid deposition on silicone hydrogel lenses, part I: quantification of oleic acid, oleic acid methyl ester, and cholesterol. *Eye Contact Lens* 2006; 32: 300-7.
13. Pucker AD, Thangavelu M, Nichols JJ. In vitro lipid deposition on hydrogel and silicone hydrogel contact lenses. *Invest Ophthalmol Vis Sci* 2010; 51: 6334-40.
14. Nichols JJ, Willcox MD, Bron AJ, Belmonte C, Ciolino JB, Craig JP, Dogru M, Foulks GN, Jones L, Nelson JD, Nichols KK, Purslow C, Schaumberg DA, Stapleton F, Sullivan DA. The TFOS International Workshop on Contact Lens Discomfort: executive summary. *Invest Ophthalmol Vis Sci* 2013; 54: TFOS7-13.
15. Jones L, Brennan NA, González-Méijome J, Lally J, Maldonado-Codina C, Schmidt TA, Subbaraman L, Young G, Nichols JJ. The TFOS International Workshop on Contact Lens Discomfort: report of the contact lens materials, design, and care subcommittee. *Invest Ophthalmol Vis Sci* 2013; 54: TFOS37-70.
16. Heynen M, Lorentz H, Srinivasan S, Jones L. Quantification of non-polar lipid deposits on senofilcon A contact lenses. *Optom Vis Sci* 2011; 88: 1172-9.
17. Fowler SA, Korb DR, Allansmith MR. Deposits on soft contact lenses of various water contents. *CLAO J* 1985; 11: 124-7.
18. Maissa CC, Franklin V, Guillon M, Tighe B. Influence of contact lens material surface characteristics and replacement frequency on protein and lipid deposition. *Optom Vis Sci* 1998; 75: 697-705.
19. Jones L, Mann A, Evans K, Franklin V, Tighe B. An in vivo comparison of the kinetics of protein and lipid deposition on group II and group IV frequent-replacement contact lenses. *Optom Vis Sci* 2000; 77: 503-10.
20. Bontempo AR, Rapp J. Protein and lipid deposition onto hydrophilic contact lenses in vivo. *CLAO J* 2001; 27: 75-80.

21. Zhao Z, Carnt NA, Aliwarga Y, Wei X, Naduvilath T, Garrett Q, Korth J, Willcox MD. Care regimen and lens material influence on silicone hydrogel contact lens deposition. *Optom Vis Sci* 2009; 86: 251-9.
22. Saville JT, Zhao Z, Willcox MDP, Blanksby SJ, Mitchell TW. Detection and quantification of tear phospholipids and cholesterol in contact lens deposits: the effect of contact lens material and lens care solution. *Invest Ophthalmol Vis Sci* 2010; 51: 2843-51.
23. Pucker AD, Nichols JJ. A method of imaging lipids on silicone hydrogel contact lenses. *Optom Vis Sci* 2012; 89: E777-87.
24. Pucker AD, Thangavelu M, Nichols JJ. Enzymatic quantification of cholesterol and cholesterol esters from silicone hydrogel contact lenses. *Invest Ophthalmol Vis Sci* 2010; 51: 2949-54.
25. Pucker AD, Nichols JJ. Analysis of meibum and tear lipids. *Ocul Surf* 2012; 10: 230-50.
26. Lorentz H, Heynen M, Khan W, Trieu D, Jones L. The impact of intermittent air exposure on lipid deposition. *Optom Vis Sci* 2012; 89: 1574-81.
27. Mirejovsky D, Patel AS, Rodriguez DD, Hunt TJ. Lipid adsorption onto hydrogel contact lens materials. Advantages of Nile red over oil red O in visualization of lipids. *Optom Vis Sci* 1991; 68: 858-64.
28. Bontempo AR, Rapp J. Lipid deposits on hydrophilic and rigid gas permeable contact lenses. *CLAO J* 1994; 20: 242-5.
29. Bontempo AR, Rapp J. Protein-lipid interaction on the surface of a hydrophilic contact lens in vitro. *Curr Eye Res* 1997; 16: 776-81.
30. Bontempo AR, Rapp J. Protein-lipid interaction on the surface of a rigid gas-permeable contact lens in vitro. *Curr Eye Res* 1997; 16: 1258-62.
31. Carney FP, Nash WL, Sentell KB. The adsorption of major tear film lipids in vitro to various silicone hydrogels over time. *Invest Ophthalmol Vis Sci* 2008; 49: 120-4.
32. Jacob JT, Levet J, Edwards TA, Dassanayake N, Ketelson H. Visualizing hydrophobic domains in silicone hydrogel lenses with Sudan IV. *Invest Ophthalmol Vis Sci* 2012; 53: 3473-80.
33. Lorentz H, Heynen M, Tran H, Jones L. Using an in vitro model of lipid deposition to assess the efficiency of hydrogen peroxide solutions to remove lipid from various contact lens materials. *Curr Eye Res* 2012; 37: 777-86.
34. Ho CH, Hlady V. Fluorescence assay for measuring lipid deposits on contact lens surfaces. *Biomaterials* 1995; 16: 479-82.
35. Hart D, Lane B, Josephson J, Tisdale R, Gzik M, Leahy R, Dennis R. Spoilage of hydrogel contact lenses by lipid deposits. Tear-film potassium

depression, fat, protein, and alcohol consumption. *Ophthalmology* 1987; 94: 1315-21.

36. Brown SH, Kunnen CM, Duchoslav E, Dolla NK, Kelso MJ, Papas EB, de la Jara PL, Willcox MD, Blanksby SJ, Mitchell TW. A comparison of patient matched meibum and tear lipidomes. *Invest Ophthalmol Vis Sci* 2013; 54: 7417-24.

37. Copley KA, Zhang Y, Radke CJ. Wettability of SCLs assessed in a model blink-cycle cell. *Invest Ophthalmol Vis Sci* 2006; 47: E-abstract 2407.

38. Jacob J, Frederick R, Tucker C, Love L. Effect of static and non-static in-vitro techniques on lipid penetration into SiHy contact lenses. *Invest Ophthalmol Vis Sci* 2013; 54:E-abstract 5486.

39. Tighe B, Franklin V. Lens deposition and spoilation. In: Larke JR, ed. *The Eye in Contact Lens Wear*, 2nd ed. Boston, MA: Butterworth-Heinemann; 1997: 49-100.

40. Kotsmar C, Sells T, Taylor N, Liu DE, Prausnitz JM, Radke CJ. Aqueous solute partitioning and mesh size in HEMA/MAA hydrogels. *Macromolecules* 2012; 45: 9177-87.

41. Cerretani CF, Ho NH, Radke CJ. Water-evaporation reduction by duplex films: application to the human tear film. *Adv Colloid Interface Sci* 2013; 197-198: 33-57.

42. Maurer SA, Bedbrook CN, Radke CJ. Cellulase adsorption and reactivity on a cellulose surface from flow ellipsometry. *Ind Eng Chem Res* 2012; 51: 11389-400.

43. Bron AJ, Tiffany JM, Gouveia SM, Yokoi N, Voon LW. Functional aspects of the tear film lipid layer. *Exp Eye Res* 2004; 78: 347-60.

44. Glasgow BJ, Gasymov OK, Abduragimov AR, Engle JJ, Casey RC. Tear lipocalin captures exogenous lipid from abnormal corneal surfaces. *Invest Ophthalmol Vis Sci* 2011; 51: 1981-7.

45. Gasymov OK, Abduragimov AR, Glasgow BJ. Evidence for internal and external binding sites on human tear lipocalin. *Arch Biochem Biophys* 2007; 468: 15-21.

46. Cerretani CF, Radke CJ. Tear dynamics in healthy and dry eyes. *Curr Eye Res* 2014; 39: 580-95.

47. Fatt I, Weissman BA. *Physiology of the Eye: An Introduction to the Vegetative Functions*, 2nd ed. Boston, MA: Butterworth-Heinemann; 1992.

48. Franklin V, Pearce E, Tighe B. Hydrogel lens spoilation—deposit formation and the role of lipids. *Optician* 1991; 202: 19-26.

49. Franklin V, Evans K, Jones L, Singh-Gill U, Tighe B. Interaction of tear lipids with soft contact lenses. *Optom Vis Sci* 1995; 72: 145-6.

50. Luensmann D, Jones L. Protein deposition on contact lenses: the past, the present, and the future. *Cont Lens Anterior Eye* 2012; 35: 53-64.
51. Liu DE, Kotsmar C, Nguyen F, Sells T, Taylor NO, Prausnitz JM, Radke CJ. Macromolecule sorption and diffusion in HEMA/MAA hydrogels. *Ind Eng Chem Res* 2013; 52: 18109-20.
52. Dursch TJ, Taylor NO, Liu DE, Wu RY, Prausnitz JM, Radke CJ. Water-soluble drug partitioning and adsorption in HEMA/MAA hydrogels. *Biomaterials* 2014; 35: 620-9.
53. Lorentz H, Heynen M, Trieu D, Hagedorn SJ, Jones L. The impact of tear film components on in vitro lipid uptake. *Optom Vis Sci* 2012; 89: 856-67.